AIChE

Preparation of Tailor-Made Polystyrene Nanocomposite with Mixed Clay-Anchored and Free Chains via Atom Transfer Radical Polymerization

Hossein Roghani-Mamaqani, Vahid Haddadi-Asl, Mohammad Najafi, and Mehdi Salami-Kalajahi
Dept. of Polymer Engineering and Color Technology, Amirkabir University of Technology, P.O. Box 15875-4413, Tehran, Iran

Mohammad Najafi and Mehdi Salami-Kalajahi
Polymer Engineering Division, Research Institute of Petroleum Industry (RIPI), 1485733111, Tehran, Iran

DOI 10.1002/aic.12395
Published online October 1, 2010 in Wiley Online Library (wileyonlinelibrary.com).

Tailor-made polystyrene nanocomposite with mixed free and clay-attached polystyrene chains was synthesized using atom transfer radical polymerization. Vinylbenzyl trimethylammonium chloride having a double bond, which could be incorporated into polystyrene chains by a grafting through process, was used as a nanoclay modifier. Conversion and molecular weight evaluation was carried out using gas chromatography and gel permeation chromatography, respectively. The thermogravimetric analysis results confirmed the elevated thermal stability of the nanocomposites in comparison with the neat polystyrene sample. Additionally, the T_g increases by clay loading was confirmed by differential scanning calorimetry (DSC). The difference in the degradation temperature of C—Br bond in attached and free polystyrene chains was well revealed in DSC thermograms. Finally, a lower clay loading resulted in an exfoliated structure as proved by X-ray diffraction and transmission electron microscopy results.
 AIChE J, 57: 1873–1881, 2011
Keywords: tailor-made polystyrene, nanocomposite, ATRP

Introduction

In recent decades, much attention has been paid on polymer/clay nanocomposites as advanced polymeric materials. Relatively low loading of clay has been resulted in significant improvements in mechanical properties,[1] thermal stability and flame retardancy,[2] magnetic and electric properties,[3] gas permeation,[4] and enhanced modulus[5] for the synergism between the components. On the contrary, the degree of dispersion of the clay platelets into the matrix determines the structure of nanocomposites and affects the aforementioned properties. Based on the reactants, processing system, and interaction between clay layers and host polymer, melt intercalation, solution blending, and in situ polymerization have been used to prepare a nanocomposite. The latter consists of polymerization of monomer in the presence of clay layers.[6] In situ polymerization almost results in exfoliated structure which is caused by the low viscosity of monomer, which brings about the easy intercalating of monomer into interlayer gallery of clay particles. Because of a variety of polymerization systems and methods, in situ polymerization is one of the most interesting techniques for nanocomposite

Correspondence concerning this article should be addressed to V. Haddadi-Asl at haddadi@aut.ac.ir.

preparation. Suspension, solution, bulk, emulsion, and miniemulsion polymerizations have been used in nanocomposite preparation via in situ polymerization.[7]

Considering the extension of different ways of polymerization, one cannot ignore the prominent role of controlled radical polymerization (CRP) in the synthesis of polymers with narrow molecular weight distribution and well-defined topology. CRP has attracted much attention over the recent years for providing simple and robust routes to the synthesis of well-defined, low-polydispersity polymers.[8] In this context, nitroxide-mediated polymerization,[9] reversible addition-fragmentation chain transfer polymerization (RAFT),[10] and atom transfer radical polymerization (ATRP)[11,12] have extensively been studied. Some advantages of ATRP over other CRP systems include the applicability to a wide variety of monomers and systems of polymerization (since its equilibrium can be easily adjusted for a given system by modifying the ligand of the catalyst),[13] the simplicity of reaction setup and conditions (low temperature and pressure), and its less sensitivity to impurities.[14] Because of living nature of ATRP, it can be used not only to synthesize homopolymers but also to prepare various kinds of functional (chain end functionality or functionality on the backbone), gradient, graft, branched, star, and brush (co)polymer structures. Functionality in both homopolymers prepared via ATRP (macroinitiator) or initiators plays a key role in synthesizing the previously mentioned structures. Also, a vast range of vinyl monomers such as styrenics,[15] acrylonitrile,[16] (meth)acrylates,[17] and vinyl acetate[18] can be synthesized by this method.

A review of related literature indicates that there are some attempts on the preparation of styrene nanocomposites via in situ polymerization. Fan et al. reported the coat of AIBN on clay platelets to initiate PMMA chains from the surface of nanoclay layers.[19] The use of vinylbenzyldimethylethanolammonium chloride as an intercalating agent of pristine montmorillonite and as an engaging agent with growing radicals for its unsaturated carbon bond was presented by Tseng et al.[20] Living anionic polymerization of styrene in the presence of clay layers was demonstrated by Zhou et al.[21] Well-defined, narrow-molecular-weight-distribution polymer nanocomposites have been prepared by nitroxide mediated polymerization (NMP),[22] RAFT polymerization,[23] ring opening metathesis polymerization (ROMP),[24] and ATRP[25] by far. In all the polymerization methods, as monomer penetrates into the intergallery of clay platelets and polymerization initiates via providing appropriate conditions, the silicate layers could be gradually pushed apart, resulting in a well-dispersed exfoliated structure. Bottcher et al. were the first to introduce ATRP as a powerful technique for preparation of grafted polystyrene on clay platelets via an esterification process. They synthesized an intercalating agent that simultaneously played the role of ATRP initiator.[25] Poly(ethylacrylate)/clay nanocomposites have been prepared by dispersing ethylacrylate in clay layers and then using in situ ATRP method to polymerize it between the intergallery distance of clay by Haimanti et al. recently.[26]

In this research, we take the advantages of ATRP method to synthesize polystyrene nanocomposite using modified montmorillonite by grafting through process. The ATRP process was applied to the mixture of monomer and modified montmorillonite, which is ion exchanged with a special chemical having structure provided in Scheme 1. In our well-tuned process, a mixture of clay-attached and free polystyrene chains was obtained. By now, there is not any clear report on differences in properties of free and clay-attached polymer chains. In this study, there is a combination of free and clay-attached polystyrene chains in the nanocomposite matrix. We have tried to investigate not only the effect of nanoclay layers on thermal properties and kinetics of polymerization but also the discrepancies in characteristic thermal and kinetics behaviors of free and attached polymer chains in the same matrix have been investigated.

The effect of clay addition on the rate constant of propagation, termination, and consequently on the properties of polymer synthesized both in free and confined state is currently ongoing in our group.

Experimental Part

Materials

Styrene (Aldrich, 99%) was passed through an alumina-filled column, dried over calcium hydride, and distilled under reduced pressure (60°C, 40 mm Hg). Na-montmorillonite (Southern clay product with a cation exchange value of 92 mequiv/100 g) was stirred in deionized water for a day and then was separated by centrifugation, filtered, dried, and finally stored in a vacuum oven (50°C, 40 mm Hg). Copper(I) bromide (CuBr, Aldrich, 98%) was washed with glacial acetic acid, filtered, and finally washed with ethanol; it was dried in a vacuum oven (50°C, 40 mm Hg) and then stored in a nitrogen atmosphere. *N,N,N′,N″,N‴*-pentamethyldiethylenetriamine (PMDETA, Aldrich, 99%), ethyl alpha-bromoisobutyrate (EBiB, Aldrich, 97%), anisole (Aldrich, 99%), vinylbenzyltrimethylammonium chloride (Aldrich, 99%), xylene (Sigma–Aldrich, 99%), and neutral aluminum oxide (Aldrich) were used as received.

Preparation of organophilic montmorillonite

A quaternary alkyl ammonium cation with a double bound at the end of its backbone was used as a pristine clay modifier. The amount of intercalating agent used for the cation-exchange reaction is calculated by[27]:CEC value of clay per 100 g $\times$ clay content (g) $\times$ 1.2 = (X/M_w of intercalating agent) $\times$ 1 $\times$ 100 where, X represents the quantity of clay modifier in gram, and the constant of 1.2 refers to using an excess amount of intercalating agent. For all the preparations, a suspension of 4.5 g of Na-MMT with a CEC value of 92 mequiv/100 g in 200 mL of distilled water was stirred in a round-bottom flask over 5 h. During the same time, in another flask, 1.05 g of intercalating agent and 200 mL ethanol were stirred for 5 h. The modifier solution in ethanol was added dropwise to the clay suspension. After the solution was stirred overnight, the white precipitated part was filtered, washed with 80/20 (v/v) methanol/water mixture several times until no chloride ion could be detected by an $AgNO_3$ solution. The product was dried in vacuum in 60°C overnight, and the yield was 92%.

Preparation of polystyrene/modified montmorillonite nanocomposite

The ATRP polymerizations were performed in a 250-mL lab reactor which was placed in an oil bath thermostated at

Table 1. The Designation of the Samples and Various Modes of Their Preparation Along with the Content of Nanoclay

Sample Designation	The Time of Monomer and Clay Dispersion (h)	Proportion of Clay (wt %)	Method of Preparation
PS	ATRP	0	–
PSNA240	In situ ATRP	2	40
PSNA400	In situ ATRP	4	0
PSNA440	In situ ATRP	4	40
PSNA840	In situ ATRP	8	40

the desired temperature. A number of batch polymerizations were run at 110°C in a solution medium and with the molar ratio of 140:1:1:1 for [M]:[EBiB]:[CuBr]:[PMDETA], giving a theoretical polymer molecular weight of 10.415 g mol^{-1} at 100% conversion. The reactor was degassed and back-filled with nitrogen gas three times, and then left under N_2. The batch experiments were run by adding deoxygenated monomer (styrene, 32.256 mL, 0.28 mol), modified montmorillonite, catalyst (CuBr, 0.287 g, 0.002 mol), ligand (PMDETA, 0.417 mL, 0.002 mol), xylene as the diluents (10 mL), and 0.5 mL of deoxygenated anisole as the internal standard to the reactor and then increasing the reaction temperature to 110°C (within about 15 min). The solution turned light green as the CuBr/PMDETA complex formed. Finally, after the majority of the metal complex had formed, initiator (EBiB, 0.293 mL, 0.002 mol) was added to the system to start the styrene ATRP. A sample was taken before the reaction started and used as a comparison reference for the samples later taken at the different stages of the reaction so as to measure the monomer conversion.

Separation of attached and unattached polymer chains

The polymer samples were dissolved in THF and passed through a neutral aluminum oxide column to remove catalyst particles. By high-speed ultracentrifugation and then passing the solution through a 0.2 micrometer filter, the unattached polymer chains were separated from the anchored ones via passing through the filter pores.[28] The remained tethered chains were cleaved from the layers by a reverse cation exchange procedure: Tethered polystyrene chains (2 g), 125 mL of THF/Methanol (4/1, v/v) solution, and LiBr (0.1 g) were refluxed in a 150 mL round-bottom flask equipped with a condenser and stirring bar for 6 h. The cleaved polystyrene samples were obtained after centrifugation. The solution was then poured into methanol (500 mL) to precipitate the polymer chains. After filtration, the cleaved polymer chains were dried in a vacuum oven in 65°C.[29]

The designation of the samples and various modes of their preparation along with the content of nanoclay are summarized in Table 1.

Gas chromatography (GC) is a simple and highly sensitive characterization method and does not require removal of the metal catalyst particles. GC was performed on an Agilent-6890N with a split/splitless injector and flame ionization detector, using a 60 m HP-INNOWAX capillary column for the separation. The GC temperature profile included an initial steady heating at 60°C for 10 min and a 10°C/min ramp from 60 to 160°C. The samples were also diluted with acetone. The ratio of monomer to anisole at the different stages of the reaction was measured by GC to calculate monomer conversion throughout the reaction. The average molecular weights and molecular weight distributions were measured by gel permeation chromatography (GPC) technique. A Waters 2000 ALLIANCE with a set of three columns of pore sizes of 10,000, 1000, and 500 Å was utilized to determine polymer average molecular weight and polydispersity index (PDI). THF was used as the eluent at a flow rate of 1.0 mL/min, and the calibration was carried out using low polydispersity polystyrene standards. For the GPC measurements, catalyst particles were removed by passing the polymer solutions through a neutral aluminum oxide column. X-ray diffraction spectra were collected on an X-ray diffraction instrument (Siemens D5000) with a Cu target ($\lambda = 0.1540$ nm) at room temperature. The system consisted of a rotating anode generator, and operated at 35 kV and a current of 20 mA. The samples were scanned from $2\theta = 2°$ to 10° at the step scan mode, and the diffraction pattern was recorded using a scintillation counter detector. Thermal analyses were carried out using a differential scanning calorimetry (DSC) instrument (NETZSCH DSC 200 F3, Netzsch Co, Selb/Bavaria, Germany). Nitrogen at a rate of 50 mL/min was used as the purging gas. Aluminum pans containing 2–3 mg of the samples were sealed using the DSC sample press. The samples were heated from ambient temperature to 220°C at a heating rate of 10°C/min. T_g was obtained as the inflection point of the heat capacity jump. Thermal gravimetric analyses were carried out with a PL thermo-gravimetric analyzer (Polymer Laboratories, TGA 1000, UK). The thermograms were obtained from ambient temperature to 550°C at a heating rate of 10°C/min. A sample weight of about 10 mg was used for all the measurements, and nitrogen was used as the purging gas at a flow rate of 50 mL/min; an empty pan was used as the reference. The transmission electron microscope, Philips EM 208, with an accelerating voltage of 200 kV was used to study the morphology of the nanocomposites; the samples of 70 nm thickness were prepared by Reichert-ultramicrotome (type OMU 3).

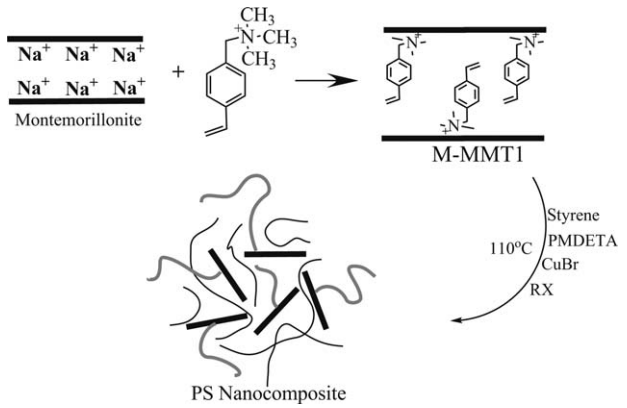

Scheme 1. Preparation of polystyrene nanocomposite.

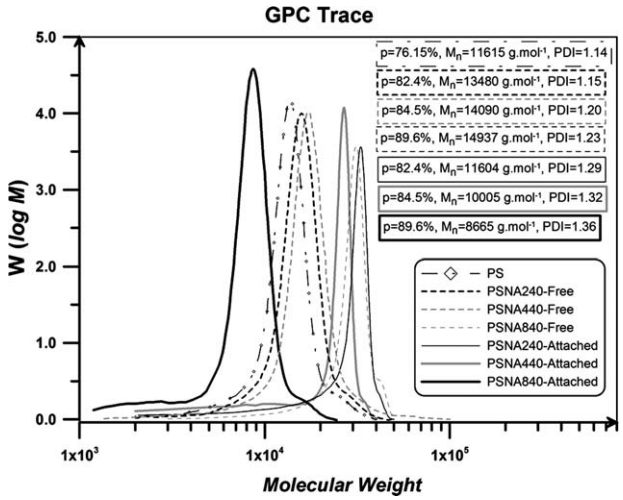

Figure 1. GPC traces of PS macroinitiator and nanocomposites prepared via ATRP.

Results and Discussion

Intercalated nanoclay with an intercalating agent, which has a double bond (M-MMT1), was used in the nanocomposite preparation through in situ ATRP; an schematic presentation is demonstrated in Scheme 1.

Figure 1 represents the results of the polymer chain characterizations of the resultant nanocomposites, namely number and weight average molecular weights and polydispersity indexes of free and clay-attached polymer chains. The GPC traces of all the samples display monomodal peaks corresponding to the molecular weight values predetermined by the molar ratio of monomer to initiator. There is a shoulder in the molecular weight distributions at high molecular weight tail, which is attributed to radical coupling.[30,31] As it is clear, the more the clay content, the more intensified the mentioned peak. Such a deviation from living feature of ATRP is on account of the acceleration effect of nanoclay on the rate of polymerization. This phenomenon is attributed to the partially polarizing effect of the nanoclay on the reaction medium and thereby its acceleration effect on the polymerization rate. As reported previously, polar solvents (especially hydroxyl containing ones like water, phenol, and carboxylic acids), also, exert a rate acceleration effect on the polymerization systems for increasing radical activation rate and reducing radical recombination rate.[32–36] Pendant hydroxyl groups and oxygen containing groups of clay layers could possibly cause a polarity change into the reaction medium. Additionally, it is evident from a recent research that a negatively charged surface could absorb and gather positively charged catalyst (Cu ions in our work) and consequently enhance the rate of chain growth.[37] The high values of initiator efficiency also signify the controlled nature of the polymerization system; additionally, it states the accelerating effect of nanoclay on the polymerization rate in styrene ATRP. The accelerating effect of nanoclay on the polymerization rate was also reported in other works.[26,38] The polydispersity index of polymer chains increases by the addition of nanoclay. The addition of nanoclay, which acts as an impurity in the polymerization system, broadens the molecular weight distribution of the resultant polymers; PDI increases from 1.14 to 1.23 by an 8 wt % loading of nanoclay. The number and weight average molecular weights of the clay-attached polystyrene chains are lower than that of the freely dispersed polystyrene chains. It is also clear that polydispersity index of attached chains is higher compared to that of the free polystyrene chains. The interlayer space of nanoclay layers confines the diffusion of lengthy dormant species into the distance between nanolayers; consequently, by diffusion of small molecules of alkyl halide and their attachment onto the clay layers, to propagate attached polystyrene chains, it is necessary that monomer diffuses into the interlayer spacing. Because the diffusion of monomer in the mentioned confined region is a slow process, the molecular weight of the polymer chains propagated from the clay layers would be lower than that of the unattached free polystyrene chains. The low activity of clay-attached polymer chains would be another reason to slow the activation process and thereby lowering the molecular weight of the attached polymer chains. High values of PDI of the attached polystyrene chains can be ascribed to the competition of the attached polymer chains to attract monomer molecules that can hardly diffuse into the interlayer space of nanoclay layer.[26] Additionally, nanoclay is considered as an impurity in the polymerization medium causes the molecular weight distribution of the extracted polymers to widen.

The nanoclay used in this research belongs to 1:2 phillosilicates. Its crystal structure consists of two-dimensional layers formed by fusing two silica tetrahedral sheets to an octahedral sheet of $Al(OH)_3$. Van der Waals forces hold the layers of nanoclay particles in the stack state with a gap between the platelets, which is called interlayer or gallery. XRD is an effective technique for determining the extent of clay dispersion ordered or disordered structure in a polymer nanocomposite matrix. Figure 2A displays the XRD patterns of the nanoclays modified by different extents of the modifier. As it is can be seen, there is no evident difference between the XRD patterns of M-MMT1 and M-MMT1.5 (the clay with the modifier content of a half higher than that of M-MMT1); this shows that the proportion of the modifier used in M-MMT1 is the optimum one that was extracted from the equation. Therefore, M-MMT1 is used as the filler in synthesizing the nanocomposies. Additionally, the diffraction angle of X-ray in the modified clays were not changed by the addition of intercalating agent content, which further clarifies that the interlayer distance is not changed by varying the modifier content. However, by the addition of intercalating agent to an optimum extent, the number of cation-exchaned sites of montmorillonite layers increased to its highest level. It is worth mentioning that the mean interlayer space of the (001) plane (d_{001}) can easily be calculated using Bragg's law of diffraction from peak position (Eq. 1).

$$d = \frac{\lambda}{2 \sin \theta} \tag{1}$$

where, d is the interlayer distance; λ is the radiation wavelength of X-ray source that is equal to 1.5405 nm, and θ is the angle of incident radiation.

Figure 2B shows the XRD patterns of the neat and modified montmorillonite, the neat polystyrene, and the prepared

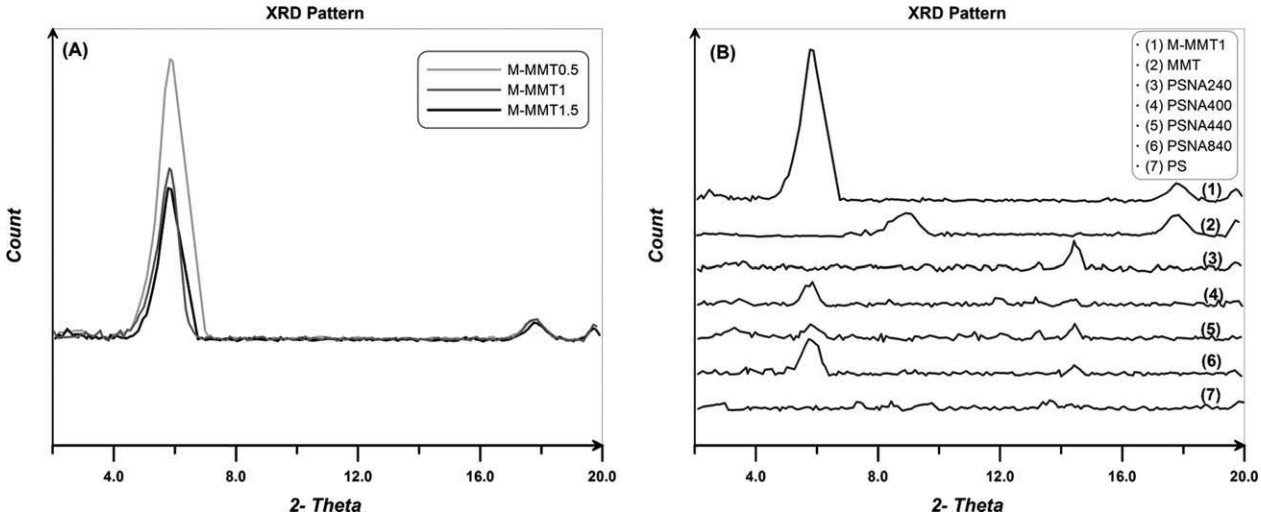

Figure 2. X-ray diffraction curves of (A) modified MMT by different amounts of modifier and (B) PS and its nanocomposites for different clay loadings in respect to 2θ.

nanocomposites in the range of $2\theta = 2$–$9°$. As it is clear, the value of d_{001} for montmorillonite is 9.74 nm ($2\theta = 9.01°$) and is increased to 15.15 nm ($2\theta = 5.81°$) in M-MMT1. This further elaborates that the intercalating process has been done successfully. There are no peaks in the X-ray pattern of the in situ synthesized nanocomposite with 2 wt % clay; however, a higher clay loading resulted in an intercalated nanocomposite structure. The disappearance of diffraction peak in PSNA240 is a result of shifting d_{001} reflection to diffraction angles smaller than 2°, which indicates that the gallery distance of the clay interlayers increases on account of increasing the polymer content between platelets. Thus, the clay is delaminated to some extent and dispersed in the polymer matrix, and therefore, an exfoliated nanocomposite is formed. However, in the case of the nanocomposites with higher amounts of clay, a weak diffraction peak at $2\theta = 5.81°$ is observed; this arises from the structure of montmorillonite modifier that has no long aliphatic tail. In comparison with the M-MMT1 diffraction peak, the lower peak area of the highly loaded nanocomposites indicates that a small amount of nanolayers remains in its stack form. However, swelling of clay layers by monomer before polymerization seems to be a prominent factor in the reduction of the amount of such a nonexfoliated clay layers. This behavior is because of the fact that by mixing monomer and clay prior to polymerization of monomer molecules, with a low viscosity, could easily penetrate into the gallery gap and expand the interlayer spacing to some extent.

The thermal stability of the specimens is studied by thermogravimetric analysis (TGA). Figure 3 illustrates typical TGA thermograms of weight loss as a function of temperature in the temperature range of 100–600°C for the neat and modified montmorillonites. In addition to the theoretical calculation of the modifier content, one can estimate the optimum amount of modifier for given nanoclay by the TGA results. As can be seen, there is not a marked difference between the M-MMT1 and M-MMT1.5 thermogravimetric graphs; however, M-MMT0.5 (the clay with the modifier content of a half lower than that of M-MMT1) and M-MMT1 shows different amounts of char. Consequently, the modifier content acquired from the equation seems to be the optimum one.

Figure 4A shows the TGA thermograms of weight loss as a function of temperature for the neat polystyrene and its nanocomposites. As it can be seen, the thermal stabilities of all the nanocomposites are higher than the neat polystyrene. By increasing the clay content of the nanocomposites, the degradation temperature rises. The 16% weight loss in M-MMT1 thermogram up to 600°C is due to the degradation of its ammonium salt modifier, and the remained portion (char) is its inorganic content. Figure 4B shows the corresponding differential thermogravimetric curves (DTG) of clay, polystyrene, and its nanocomposites for different clay loadings. It is clear that the addition of clay nanoparticles to polystyrene retards the degradation of the samples, which is ascribed to the hindrance effect of nanoplatelets on the movement of polymer chains. Below 140°C, M-MMT1.5 experiences the

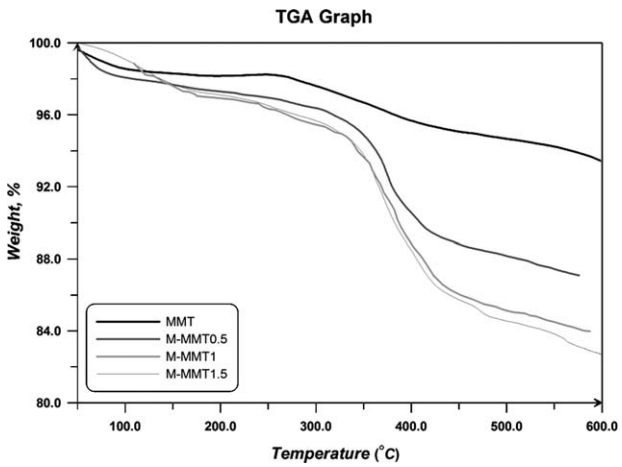

Figure 3. TGA thermograms of neat montmorillonite and modified nanoclay for different amounts of modifier.

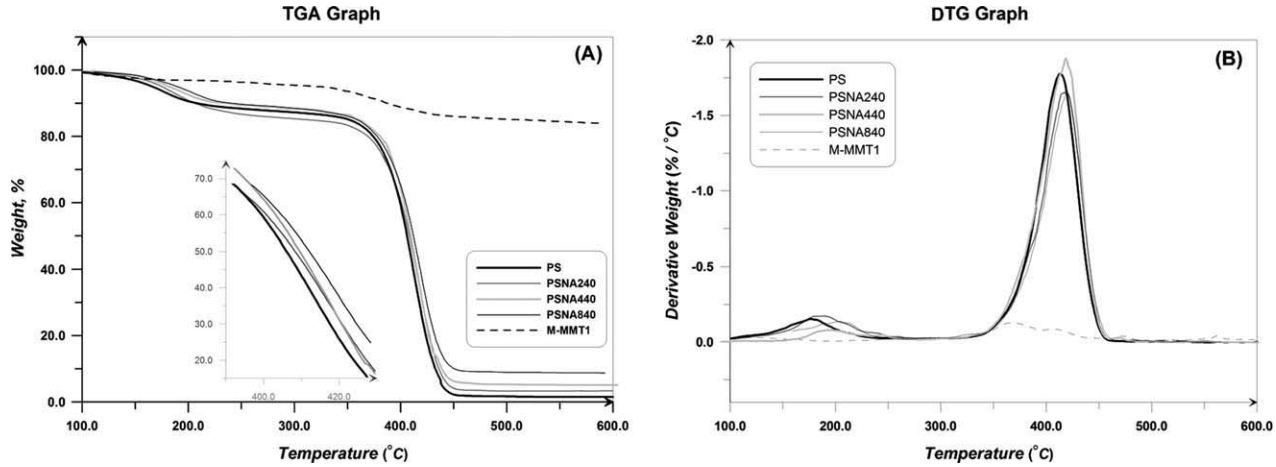

Figure 4. (A) TGA thermograms and (B) DTG thermograms of PS and its nanocomposites for different clay loadings.

least drop in its weight, which is attributed to the more hydrophobic behavior of this type of nanoclay on account of its high modifier content.[39]

The TGA data summarized in Table 2 show the temperature threshold at which the 5, 10, and 50% of the polymer degradation is occurred. In the nanocomposites, it is obvious that the degradation temperature is lower for smaller amounts of clay and increases by increasing the amount of clay. Additionally, the amount of char rises as the percentage of clay increases. Except for the degradation of the volatile parts, in the temperature range of 150–250°C, the degradation of all the samples takes place in one step and char is left after complete degradation in all the cases; the char consists of the transition metal that plays the role of catalyst in ATRP and the nanoclay. The subtraction of the char in PS samples from the char in the other samples could provide a good estimation of the percentage of clay in that sample. The degradation of the neat polystyrene occurs in the temperature window of 322–460°C; however, the nanocomposite samples exhibit a temperature window of 328–421°C for degradation. Pristine montmorillonite was found to have ~6.54% volatile materials, most of which decomposes in the temperature window of 250–450°C. After intercalation with modifier, the modified clays were analyzed, and it was found that 10.25% of M-MMT0.5 is composed of double bond containing ammonium salt; this indicates that 62.8% of sodium ions of MMT were exchanged with modifier. The proportion of ammonium cation in M-MMT1 is 13.05% which corresponds to 80.06% of ion exchange. 88.28% of sodium cations are exchanged with ammonium cations in M-MMT1.5 indicating that 14.39% of the nanoclay is composed of double bond containing modifier.

The effect of chain confinement due to clay steric hindrance can be evaluated by comparing T_g values of the neat polystyrene, PS, and clay-loaded polystyrene nanocomposites using a differential scanning calorimeter. Figure 5 depicts some information on the thermal behavior of PS and its nanocomposites. The temperature window of 25–250°C is used to describe the DSC results. For all the samples, it is found out that the clay layers do not undergo any transitions in the experiment temperature window; therefore, only thermal transitions in polystyrene are observed. The sample in DSC is also cooled to room temperature to distinguish the phase conversion and other irreversible thermal behaviors. In the heating procedure, apart from the initial unstable results, an inflection in addition to a peak point is appeared. The temperature at which the inflection happens is the T_g of the samples. Nevertheless, there are not any peaks during the cooling path, which indicates that the samples have not gone through melting or other reversible thermal evolutions. Thus, the exothermic peak is a result of C—Br bond cleavage. The temperature at which the cleavage of C—Br bond occurs further demonstrates the catalytic role of nanoclay in the ATRP reaction. There is a shoulder at temperatures higher than the peak point in the DSC curve which seems to become stronger by increasing the amount of clay. This shoulder is

Table 2. Thermal Characteristics of the Neat PS and its Nanocomposites for Different Clay Loadings

	TGA					DTG Peak		
Sample Designation	$T_{0.05}$	$T_{0.1}$	$T_{0.5}$	Char (%)	Estimated Clay Content (%)	Start (°C)	Peak (°C)	End (°C)
PS	166	206	406	1.53	0	322	413	460
PSNA240	174	208	408	3.31	1.78	328	416	465
PSNA440	181	237	410	5.17	3.64	329	419	467
PSNA840	189	241	412	9.04	7.51	334	421	476
MMT	459	–	–	93.46	–	–	–	–
M-MMT0.5	348	409	–	87.07	–	295	374	469
M-MMT1	325	387	–	83.98	–	289	372	455
M-MMT1.5	324	382	–	82.74	–	285	366	454

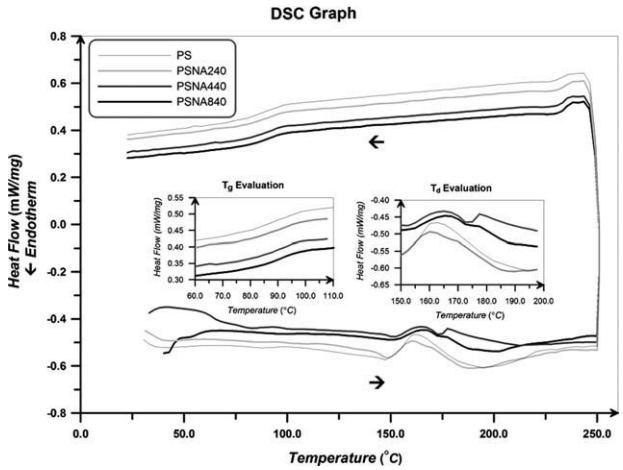

Figure 5. DSC thermogram of PS and PSN420.

attributed to the cleavage of C—Br bond of the clay-attached polymer chains.

Table 3 summarizes the T_g values, the C—Br degradation temperature, and required energy for C—Br cleavage in the polystyrene and its nanocomposites. A polystyrene sample synthesized by anionic polymerization[40] is used to compare with the samples synthesized by ATRP. According to the fact that narrow-molecular-weight-distribution polymer chains are usually synthesized via anionic polymerization, the ATRP-synthesized polystyrene and anionically synthesized polystyrene should have nearly similar T_gs if they have the same molecular weight; Table 3 confirms this deduction. By increasing the content of clay, the glass transition temperature of the samples rises, which is a result of the confinement effect of nanoclay. The rigid two-dimensional clay platelets exert a confinement on the steric mobility of chains, and hence the motions of molecule segments, which cause the inflection in the DSC curves, start at higher temperatures.

Table 3. T_g Values, the C—Br Degradation Temperature, and the Energy Required for the Dissociation of C—Br Bond in Polystyrene and Its Nanocomposites

Sample Designation	Molecular Weight (g mol^{-1})	T_g (°C)	T_d (°C) First	T_d (°C) Shoulder	ΔH_d (J g^{-1})
PS	12,685	83.3	160.3	–	14.41
PSNA240	13,480	92.4	161.2	170	10.41
PSNA440	14,090	93.8	164.7	177.8	9.251
PSNA840	14,937	93.9	166.1	176.4	6.243
Anionic PS[40]	15,020	93	–	–	–

Additionally, by adding clay, the C—Br cleavage is hindered because of the hindrance effect of nanoclay platelets. Indeed, the thermal resistance of C—Br bonds increases by the addition of nanoclay; also, the C—Br cleavage peak is diminished. It is clear that the addition of clay reduces the portion of polymer chains in a certain amount of the samples, and therefore, the number of C—Br bonds decreases; thus, a smaller amount of energy is required to dissociate these bonds. Table 3 also shows that C—Br bonds in the attached polymer chains degrade at a higher temperature compared to the free chains; this further confirms the heat hindrance effect of nanoclay platelets.

TEM images displayed in Figure 6 are used to investigate the clay platelets delamination and dispersion in the matrix of the polystyrene nanocomposites. The TEM results coincide with the aforementioned XRD data and show the complete exfoliation of clay layers in the polymer matrix of the polystyrene nanocomposite containing the lowest amount of nanoclay (PSNA240). The exfoliated clay platelets are specified by the tactoids in the TEM image (Figure 6A). However, the polystyrene nanocomposite with a higher clay loading exhibits intercalated morphology (Figure 6B). The light and dark areas represent PS matrix and silicate layers, respectively. The interlayer expansion and disordered standing of the clay layers clearly

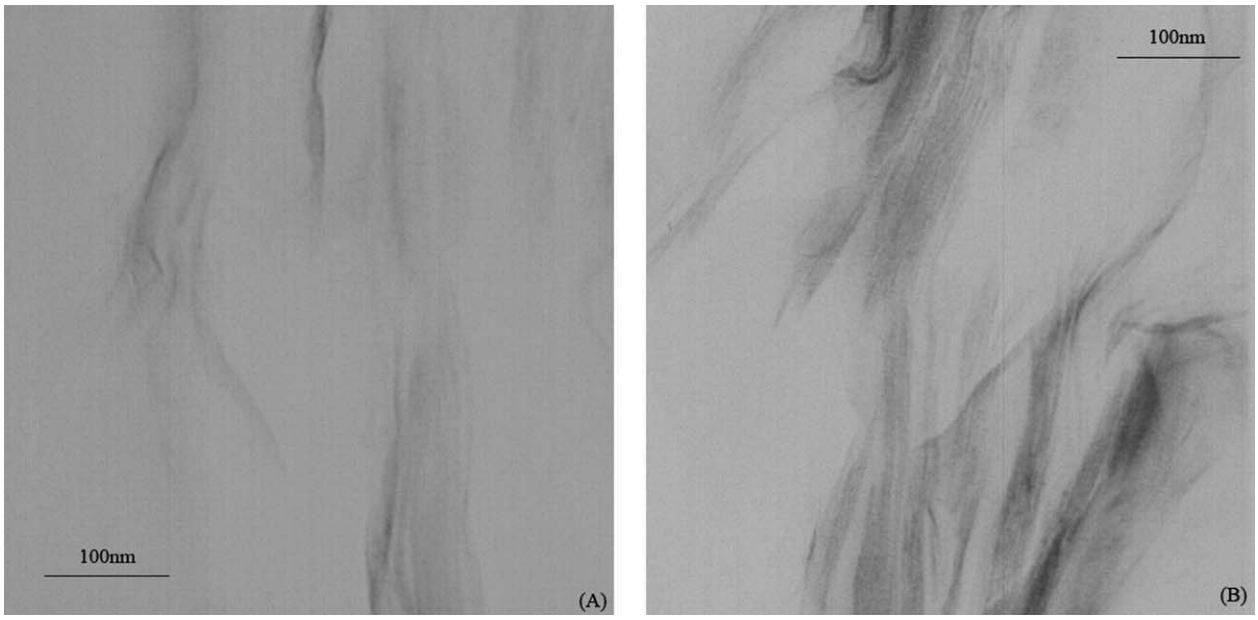

Figure 6. TEM images of (A) PSNA240 and (B) PSNA840.

show the exfoliation of the clay layers with polymer chains. The lack of space between the clay platelets and the polymer matrix confirms that M-MMT1 is compatible with the polystyrene matrix to some extent; this is because of the phenyl ring on its modifier (ammonium salt) structure.

Conclusions

ATRP was used to synthesize polystyrene and its nanocomposites with different clay loadings. The in situ prepared nanocomposites with a low amount of clay have an exfoliated structure of clay in the polymer matrix; conversely, higher amounts of clay results in an intercalated structure. The GPC traces of all the samples display a monomodal peak. Nanoclay exerts a positive effect on the rate of the polymerization of free polystyrene chains. The polydispersity index of polymer chains increases by the addition of nanoclay. Additionally, the number and weight average molecular weights of clay-attached polystyrene chains are lower than that of the freely dispersed polystyrene chains. Polydispersity index of the attached chains is higher compared to the free polystyrene chains. The XRD patterns also show that the proportion of modifier used in M-MMT1 is the optimum one. Furthermore, the diffraction angle of X-ray in the modified clays do not change by the addition of intercalating agent content, which further clarifies that the interlayer distance does not change by varying modifier content. Swelling of clay layers by monomer before the polymerization seems to be a prominent factor in the reduction of the amount of nonexfoliated clay layers. The thermal stabilities of all the nanocomposites are higher than the neat polystyrene. Also, by increasing the clay content of the nanocomposites the degradation temperature rises; the addition of clay nanoparticles to polystyrene retards the degradation of samples. There is a shoulder at temperatures higher than the peak point in the DSC curves which is attributed to the cleavage of the C—Br bond of the clay-attached polymer chains. Moreover, by increasing the amount of clay, the glass transition temperature of the samples rises, the C—Br cleavage is hindered, and the C—Br cleavage peak is diminished. Finally, the TEM results coincide with the XRD data and show the complete exfoliation of the clay layers in the polymer matrix of polystyrene nanocomposite containing the lowest amount of nanoclay (PSNA240). However, higher clay loadings result in an intercalated morphology.

Acknowledgment

Iran Petrochemical Research and Technology Company is gratefully acknowledged for its financial support (Grant# 0870128706).

Literature Cited

1. Fujimori A, Ninomiya N, Masuko T. Structure and mechanical properties in drawn poly(L-lactide)/clay hybrid films. *Polym Adv Technol.* 2008;19:1735–1744.
2. Jang BN, Costache M, Wilkie CA. The relationship between thermal degradation behavior of polymer and the fire retardancy of polymer/clay nanocomposites. *Polymer.* 2005;46:10678–10687.
3. Caruso F, Spasova M, Susha A, Giersig H, Caruso RA. Magnetic nanocomposite particles and hollow spheres constructed by a sequential layering approach. *Chem Mater.* 2001;13:109–116.
4. Nazarenko S, Meneghetti P, Julmon P, Olson B, Qutubuddin S. Gas barrier of polystyrene montmorillonite clay nanocomposites: effect of mineral layer aggregation. *J Polym Sci: Part B: Polym Phys.* 2007;45:1733–1753.
5. Shia D, Hui CY, Burnside SD, Giannelis EP. An interface model for the prediction of Young's modulus of layered silicate-elastomer nanocomposites. *Polym Compos.* 1998;19:608–617.
6. Roghani-Mamaqani H, Haddadi-Asl V, Najafi M, Salami-Kalajahi M. Synthesis and characterization of clay dispersed polystyrene nanocomposite via atom transfer radical polymerization. *Polym Compos.* In press.
7. Wang D, Zhu J, Yao Q, Wilkie CA. A Comparison of various methods for the preparation of polystyrene and poly(methyl methacrylate) clay nanocomposites. *Chem Mater.* 2002;14:3837–3843.
8. Cunningham MF. Living/controlled radical polymerizations in dispersed phase systems. *Prog Polym Sci.* 2002;27:1039–1067.
9. Georges MK, Veregin RPN, Kazmaier PM, Hamer GK. Narrow molecular weight resins by a free-radical polymerization process. *Macromolecules.* 1993;26:2987–2988.
10. Smulders W, Jones CW, Schork FJ. Continuous RAFT miniemulsion polymerization of styrene in a train of CSTRs. *AIChE J.* 2005;51:1009–1021.
11. Kamigaito M, Ando T, Sawamoto M. Metal-catalyzed living radical polymerization. *Chem Rev.* 2001;101:3689–3746.
12. Najafi M, Roghani-Mamaqani H, Salami-Kalajahi M, Haddadi-Asl V. A comprehensive Monte Carlo simulation of styrene atom transfer radical polymerization. *Chin J Polym Sci.* 2010;28:483–497.
13. Matyjaszewski K, Xia J. Atom transfer radical polymerization. *Chem Rev.* 2001;101:2921–2990.
14. Jakubowski W, Matyjaszewski K. Activators regenerated by electron transfer for atom-transfer radical polymerization of (meth)acrylates and related block copolymers. *Angew Chem Int Ed Engl.* 2006;118:4594–4598.
15. Qiu J, Matyjaszewski K. Polymerization of substituted styrenes by atom transfer radical polymerization. *Macromolecules.* 1997;30:5643–5648.
16. Matyjaszewski K, Jo SM, Paik H, Gaynor SG. Synthesis of well-defined polyacrylonitrile by atom transfer radical polymerization. *Macromolecules.* 1997;30:6398–6400.
17. Shen Y, Zhu Sh. Continuous atom transfer radical block copolymerization of methacrylates. *AIChE J.* 2002;48:2609–2619.
18. Tang H, Radosz M, Shen Y. Atom transfer radical polymerization and copolymerization of vinyl acetate catalyzed by copper halide/terpyridine. *AIChE J.* 2009;55:737–746.
19. Fan X, Xia C, Advincula R. On the formation of narrowly polydispersed PMMA by surface initiated polymerization (SIP) from AIBN-coated/intercalated clay nanoparticle platelets. *Langmuir.* 2005;21:2537–2544.
20. Tseng C, Wu J, Lee H, Chang F. Preparation and characterization of polystyrene–clay nanocomposites by free-radical polymerization. *J Appl Polym Sci.* 2002;85:1370–1377.
21. Zhou Q, Fan X, Xia C, Mays J, Advincula R. Living anionic surface initiated polymerization (SIP) of styrene from clay surfaces. *Chem Mater.* 2001;13:2465–2467.
22. Fujii S, Armes SP. Polystyrene–silica nanocomposite particles via alcoholic dispersion polymerization using a cationic azo initiator. *Langmuir.* 2006;22:4923–4927.
23. Salem N, Shipp DA. Polymer-layered silicate nanocomposites prepared through in-situ reversible addition–fragmentation chain transfer (RAFT) polymerization. *Polymer.* 2005;46:8573–8581.
24. Lahann J, Langer R. Surface-initiated ring-opening polymerization of E-caprolactone from a patterned poly(hydroxymethyl-*p*-xylylene). *Macromol Rapid Commun.* 2001;22:968–971.
25. Bottcher H, Hallensleben ML, Nu S, Wurm H, Bauer J, Behrens P. Organic/inorganic hybrids by 'living'/controlled ATRP grafting from layered silicates. *J Mater Chem.* 2002;12:1351–1354.
26. Haimanti D, Singha NK, Bhowmick AK. Structure and properties of tailor-made poly(ethyl acrylate)/clay nanocomposites prepared by in-situ atom transfer radical polymerization. *J Appl Polym Sci.* 2008;108:2398–2407.
27. Yeh JM, Liou SJ, Lin CG, Chang YP, Yu YH, Cheng CF. Effective enhancement of anticorrosive properties of polystyrene by polystyrene–clay nanocomposite materials. *J Appl Polym Sci.* 2004;92:1970–1976.
28. Akelah A, Rehab A, Agag T, Betiha M. Polystyrene nanocomposite materials by in situ polymerization into montmorillonite–vinyl monomer interlayers. *J Appl Polym Sci.* 2007;103:3739–3750.

29. Zhao H, Argoti S, Farrel P, Shipp A. Polymer-silicate nanocomposites produced by in situ atom transfer radical polymerization. *J Polym Sci Part A: Polym Chem.* 2004;42:916–924.
30. Wittmer JP, Cates ME, Johner A, Turner MS. Diffusive growth of a polymer layer by in situ polymerization. *Europhys Lett.* 1996;33:397–402.
31. Yoshikawa C, Goto A, Fukuda T. Reactions of polystyrene radicals in a monomer-free atom transfer radical polymerization system. *e-Polymers.* 2002;013:1–12.
32. Wang XS, Armes SP. Facile atom transfer radical polymerization of methoxy-capped oligo (ethylene glycol) methacrylate in aqueous media at ambient temperature. *Macromolecules.* 2000;33:6640–6647.
33. Haddleton DM, Heming AM, Kukulji D, Duncalf DJ, Shooter AJ. Atom transfer polymerization of methyl methacrylate. Effect of acids and effect with 2-bromo-2-methylpropionic acid initiation. *Macromolecules.* 1998;31:2016–2018.
34. Wang XS, Luo N, Ying SK. Controlled/living polymerization of MMA promoted by heterogeneous initiation system (EPN-X-CuX-bpy). *J Polym Sci Part A: Polym Chem.* 1999;37:1255–1263.
35. Matyjaszewski K, Nakagawa Y, Jasieczek CB. Polymerization of *n*-butyl acrylate by atom transfer radical polymerization. Remarkable effect of ethylene carbonate and other solvents. *Macromolecules.* 1998;31:1535–1541.
36. Chatterjee U, Jewrajka SK, Mandal BM. The beneficial effect of small amount of water in the ambient temperature atom transfer radical homo and block co-polymerization of methacrylates. *Polymer.* 2005;46:1575–1582.
37. Kizhakkedathu JN, Brooks DE. Synthesis of poly(*N*,*N*-dimethylacrylamide) brushes from charged polymeric subsurfaces by aqueous ATRP: effect of surface initiator concentration. *Macromolecules.* 2003;36:591–598.
38. Haimanti D, Nikhil S, Anil B. Beneficial effect of nanoclay in atom transfer radical polymerization of ethyl acrylate: a one pot preparation of tailor-made polymer nanocomposite. *Macromolecules.* 2008;41:50–57.
39. Karesoja M, Jokinen H, Karjalainen E, Pulkkinen P, Torkkeli M, Soininen A, Ruokolainen J, Tenhu H. Grafting of montmorillonite nano-clay with butyl acrylate and methyl methacrylate by atom transfer radical polymerization: blends with poly(BuA-*co*-MMA). *J Polym Sci: Part B: Polym Chem.* 2009;47:3086–3097.
40. Savin DA, Pyun J, Patterson GD, Kowalewski T, Matyjaszewski K. Synthesis and characterization of silica-graft-polystyrene hybrid nanoparticles: effect of constraint on the glass-transition temperature of spherical polymer brushes. *J Polym Sci: Part B: Polym Phys.* 2002;40:2667–2676.

Manuscript received May 7, 2010, and revision received July 14, 2010.